Molecular Crystals and Liquid Crystals
Publication details, including instructions for authors and subscription information:
http://www.tandfonline.com/loi/gmcl20

Read-Out Frequency Response of Solution-Processed Organic Photoconductive Devices

Takeshi Fukuda [a], Mitsuo Komoriya [a], Ryotaro Mori [a], Zentaro Honda [a], Khorou Takahashi [a] & Norihiko Kamata [a]

[a] Graduate School of Science and Engineering, Saitama University, Sakura-ku, Saitama-shi, Saitama, Japan

Version of record first published: 25 Jun 2009

To cite this article: Takeshi Fukuda, Mitsuo Komoriya, Ryotaro Mori, Zentaro Honda, Khorou Takahashi & Norihiko Kamata (2009): Read-Out Frequency Response of Solution-Processed Organic Photoconductive Devices, Molecular Crystals and Liquid Crystals, 504:1, 212-222

To link to this article: http://dx.doi.org/10.1080/15421400902950212

Mol. Cryst. Liq. Cryst., Vol. 504, pp. 212–222, 2009
Copyright © Taylor & Francis Group, LLC
ISSN: 1542-1406 print/1563-5287 online
DOI: 10.1080/15421400902950212

Read-Out Frequency Response of Solution-Processed Organic Photoconductive Devices

Takeshi Fukuda, Mitsuo Komoriya, Ryotaro Mori, Zentaro Honda, Khorou Takahashi, and Norihiko Kamata
Graduate School of Science and Engineering, Saitama University,
Sakura-ku, Saitama-shi, Saitama, Japan

A solution-processed organic photoconductive device sensitive to the only blue-light was demonstrated using poly(9,9-dioctylfluorene-alt-benzothiadiazole) (F8BT). The spectral selectivity was good enough to divide the incident light into a blue component, indicating the possibility of color separation without a prism for video cameras in combination with green- and red-sensitive devices. The maximum conversion efficiency of 190 μA/W was observed while irradiating the blue-light (475 nm) and applying the voltage (2.4 V). In addition, the response speed of more than 30 Hz was achieved, and it was fast enough to apply this photoconductive device to practical applications.

Keywords: color selectivity; frequency response; photoconductive device; polymer; wet process

INTRODUCTION

Recently, there have been considerable interests in organic devices [1–5] due to the possibility of solution process, which leads us to a large-device area and a low-fabrication cost. Especially, there has been an extensive effort to investigate organic light-emitting diodes, which are already practical use in main- and sub-displays for mobile phones [6]. In addition, organic photoconductive devices have been also expected for many applications, such as organic solar cells [7,8] and flexible scanners [9,10].

The part of this work was supported by "Development of functional optical materials and devices for next generation in frontier photonics," Regional New Consortium of Ministry of Economy, Trade and Industry.

Address correspondence to Takeshi Fukuda, Graduate School of Science and Engineering, Saitama University, 255 Shimo-Okubo, Sakrua-ku, Saitama-shi, Saitama 338-8570, Japan. E-mail: fukuda@fms.saitama-u.ac.jp

In previous papers, a new type of an organic image sensor overlaid with three kinds of organic photoconductive films was proposed and this device is individually sensitive to only one of the primary color components (blue, green, and red lights, respectively) [11,12]. Organic materials have singular characteristics of the absorption spectrum at a visible wavelength region [11], and the particular large absorbance leads us to realize color-selectivity in photoconductive devices by stacking several organic layers with different absorption bands [12]. Therefore, organic image sensors have attracted much attention from viewpoints of lightweight and thinness compared to such other conventional image sensors, complementary metal-oxide-semiconductor sensors and charge-coupled devices.

In order to obtain a color picture image using an organic photoconductive film, a practical read-out frequency response as well as the static sensitivity is desirable. In general, organic devices consist of stacked thin organic layers because of its lower carrier mobility than that of semiconductor materials [13,14]. Therefore, the larger capacitance of an organic layer causes the lower frequency response [15,16].

By now, previous studies have focused on frequency responses of organic devices [17–20], and the modulation frequency over MHz has been achieved. The required modulation frequency of image sensors is several tens Hz, which is over the TV flame rate. Therefore, frequency response of previous organic devices is considered to be high enough for image sensing applications. However, little is known about the read-out frequency response of an organic photoconductive device with the read-out circuit.

The primary purpose of this study is to investigate static optical characteristics of a blue-sensitive organic photoconductive device fabricated by a solution process, such as the absorption spectrum, the photocurrent spectrum, and the optical-electrical conversion efficiency while applying the blue-, green-, and red-lights, respectively. Another purpose is to estimate the frequency response of optical-electrical conversion efficiency as a function of the optical intensity of irradiated light to the organic layer.

EXPERIMENTAL

Figure 1 represents a cross sectional view of a blue-sensitive photoconductive device. This device was fabricated by spin-coating and thermal evaporation processes for an organic layer and a metal cathode, respectively. When, the blue-light is irradiated through a glass substrate and a transparent anode, an organic photoconductive layer generates carriers and read out signals are taken out from an indium

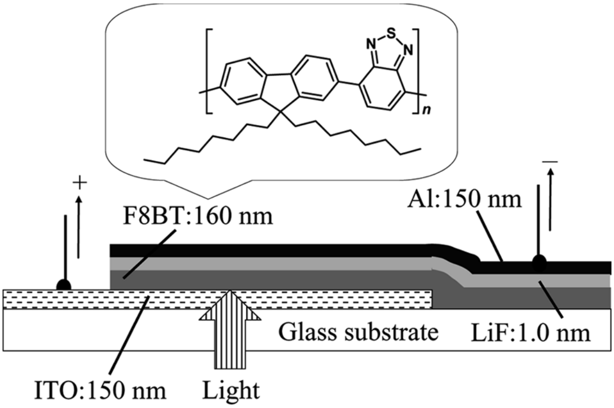

FIGURE 1 The structure of a blue-sensitive device and the molecular structure of F8BT used as a photoconductive layer.

tin oxide (ITO) anode and an Al cathode. In order to realize high device performances, the large absorption coefficient and the high carrier mobility of an organic material are necessary. Therefore, we selected poly(dioctylfluorenyl-co-benzo-thiadiazole (F8BT) as an organic photoconductive material due to its high carrier mobility [21,22]. The molecular structure of F8BT is shown in the inset of Figure 1.

At first, a glass substrate covered with a patterned ITO was cleaned with organic solvents and deionized water. The ITO layer was deposited by a conventional sputtering method, and the thickness was 150 nm. A blue-sensitive organic photoconductive material of F8BT was dissolved in chloroform as a content of 15 g/l. After passing through a filter with 0.45 μm holes, the organic solution was spin-coated at a rotation speed of 1000 rpm for 60 sec. And then, chloroform was removed by baking the sample in nitrogen atmosphere at 100 degree for 10 min. Finally, LiF and Al were thermally evaporated successively on the top of an organic layer. The device structure was Glass/ITO (150 nm)/F8BT (160 nm)/LiF (1.0 nm)/Al (150 nm), and the photoconductive area was 6.25 mm^2.

The ultraviolet-visible light absorption spectrum of the F8BT neat film was recorded with a double-beam UV/Vis spectrophotometer (V-550, JASCO). In addition, the photocurrent spectrum of the device was estimated by measuring the wavelength dependence of photocurrent density while irradiating the monochromic light by a fluorescence spectrometer (FP-777, JASCO). The irradiated light was modulated by an optical chopper, and the photocurrent was detected by a digital lock-in amplifier (LI5640, NF Corporation).

The quantum efficiency, defined as the number of output electrons divided by the total number of irradiated photons, was estimated from the measured photocurrent and the optical intensity of irradiated light. In order to estimate the color-selectivity of this device, we used three-kinds of light-emitting diodes (LEDs) with center wavelengths of 469, 525, and 619 nm, respectively. In addition, the dark current was also measured without irradiating light.

In order to investigate transient responses of the fabricated device, we measured the step response and the transient voltage characteristics while applying the pulse voltage to a read-out circuit. The electronic circuit of a measurement setup is shown in Figure 2(a). In addition, Figure 2(b) shows a fabricated read-out circuit for the organic

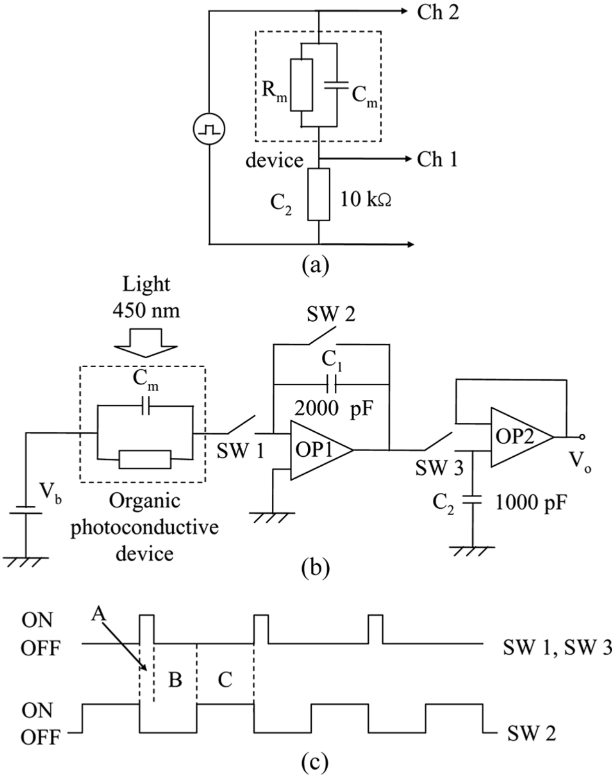

FIGURE 2 (a) The electric circuit to measure transient properties of an organic photoconductive device. (b) The read-out circuit for an organic photoconductive device and (c) the timing chart of SWs (SW 1, 2, and 3) used in the read-out circuit.

photoconductive device. The read-out circuit was fabricated in combination with several electronic equipments, operational amplifiers (OP 1 and OP 2), analog switches (SW 1, SW 2, and SW 3), and several capacitances. When the excitation light with the center wavelength of 450 nm was irradiated the photoconductive device, the photocurrent was measured as an output voltage of V_o.

Figure 2(c) indicates the timing chart of switches, SW 1, SW 2, and SW 3. If SWs 1 and 3 are closed in the time region A, the capacitance of the organic photoconductive layer (C_m) is charged up to V_b. Then, the charging current corresponding to the photocurrent transports through SW1, and is integrated with the aid of the capacitance of integrator (C_1). The output voltage of OP1 is sampled and held in the capacitance (C_2) as the read out voltage of V_o. After closing the SW 2, the integrated charge in the capacitor (C_1) is discharged and reset in the case of the region C shown in Figure 2(c). Therefore, the photocurrent of the organic photoconductive device can be read sequentially by opening and closing these analog SWs.

RESULTS AND DISCUSSION

The dotted curve in Figure 3 shows the absorption spectrum of the F8BT neat film. The peak wavelength and the full width at half maximum (FWHM) were 463 and 85 nm, respectively. The maximum

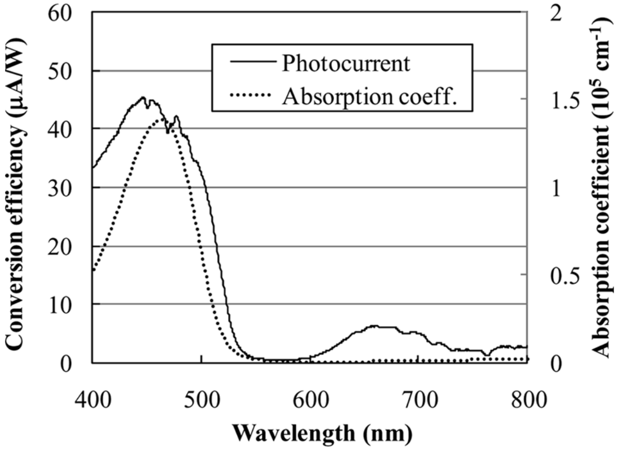

FIGURE 3 The photocurrent spectrum of the organic photoconductive device under the bias voltage of 2.5 V and the absorption spectrum of the F8BT neat film.

absorption coefficient was $1.38 \times 10^5\,\mathrm{cm}^{-1}$, corresponding to the absorbance of 80.2% through the organic layer of 160 nm. Therefore, the most of incident light is absorbed into the F8BT layer, and photo-induced carriers are considered to be excited efficiently. However, the thickness is not optimized yet, and the higher absorbance is necessary to improve the device performance. However, the F8BT layer over 160 nm is difficult to coat using the spin coating process owing to the low concentration of organic solution.

The photocurrent spectrum of the device is also shown by the solid curve in Figure 3. Here, the bias voltage of 2.5 V was applied to the device. The spectral shape is similar to the absorption spectrum of the F8BT neat film. Furthermore, the spectral photo-response curve had respective peak wavelength at 456 nm, which was near the value at the absorption peak. Therefore, these results clearly indicate that a selectively only blue-sensitive organic photoconductive device has been achieved by the wet process. However, only the photocurrent spectrum showed second peak at the red wavelength region. In order to investigate the second peak of the photocurrent spectrum, we measured the PL spectrum of the device excited at 456 nm corresponding to the first peak of the photocurrent spectrum. However, the measured PL spectrum had no peak at the red wavelength region. Although the reason is not well confirmed at this stage, we consider it to be unessential from the viewpoint of the absorption spectrum in Figure 3. We tried to improve the quality of the organic layer and metal electrode.

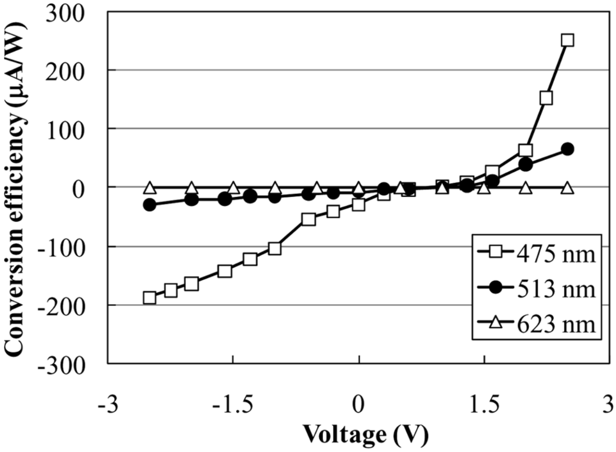

FIGURE 4 The relationship between the conversion efficiency of the organic photoconductive device and the applied voltage while irradiating the blue (475 nm), green (513 nm), and red (623 nm) lights, respectively.

Figure 4 shows conversion efficiency-voltage characteristics of the photoconductive device while irradiating blue- (475 nm), green- (513 nm), and red- (623 nm) lights, respectively. By excitation of the blue-light, the conversion efficiency of the photoconductive device was 250 μA/W, while those were 64.8 and 0.007 μA/W for green- and red-excitations, respectively. Since the higher absorption coefficient of an organic material causes the large conversion efficiency of a photoconductive device, this property change is primarily associated with photocurrent and absorption spectra as shown in Figure 3.

The conversion efficiency increased with increasing the applied voltage in all the cases of irradiated lights. This is because the carrier mobility of organic materials increased with increasing the voltage [23], resulting in the efficient carrier transfer in F8BT with less recombination probability. As a result, the conversion efficiency improves at higher electric field.

Photocurrent and dark-current are plotted in Figure 5. The intensity and the center wavelength of irradiated light were 2.8 mW/cm^2 and 475 nm, respectively. As clearly shown in Figure 5, the photocurrent exceeded the dark current by two orders of magnitude in all the cases of applied voltage.

We estimated capacitance and resistance of an organic photoconductive layer (F8BT) by measuring step response and transient voltage characteristics. Figure 6(a) shows the transient output voltage of Ch 1 and 2. Here, the output voltage characteristics of Ch 1 and 2

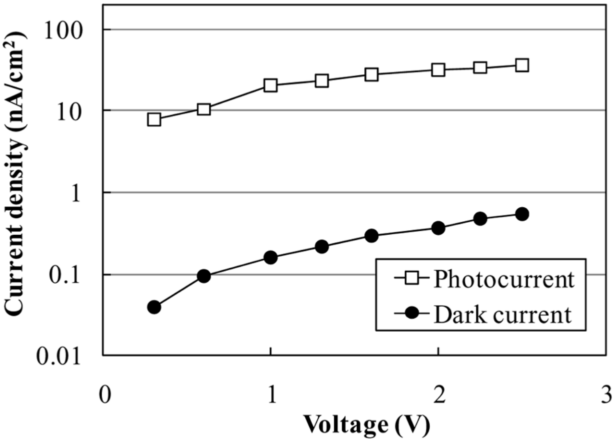

FIGURE 5 Photocurrent and dark current as a function of the applied voltage. The center wavelength and the intensity of irradiated light were 475 nm and 2.8 mW/cm^2, respectively.

are corresponding to the photocurrent and the applied voltage. In addition, the center wavelength of irradiated light was 450 nm, which is near the value of absorption peak, as shown in Figure 3. When the applied voltage of Ch 2 is turned off, the photocurrent increases gradually. The time required to change the output voltage to 63.2% of full change gave a rise time of 23 μs. From the rise time, the capacitance value of $C_m = 3.7 \times 10^4\,pF/cm^2$ was derived.

Figure 6(b) shows the transient voltage characteristics of Ch 1 while applying the pulse voltage. This experimental result yields the voltage

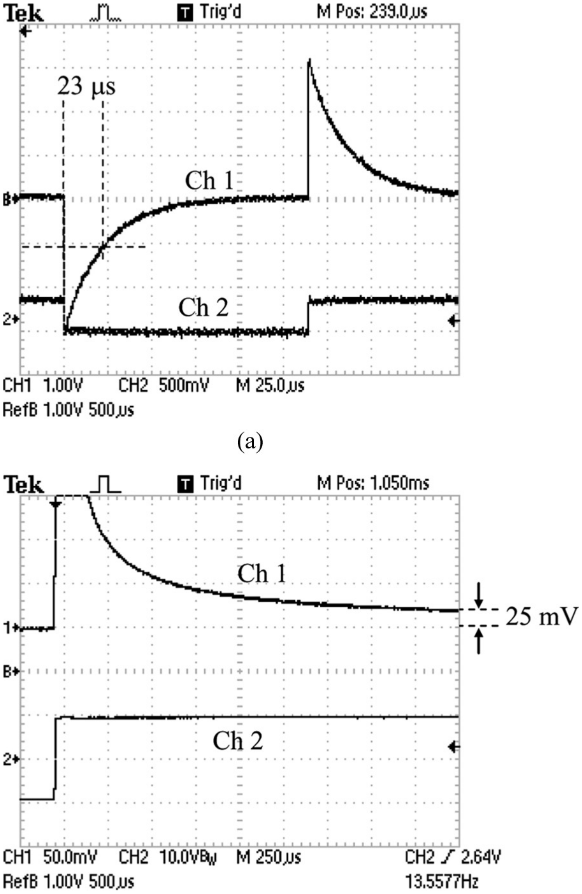

(a)

(b)

FIGURE 6 (a) The photoccurent (Ch 1) and applied voltage (Ch 2) of organic photoconductive device and (b) the transient voltage characteristic while applying the pulse voltage to Ch 2.

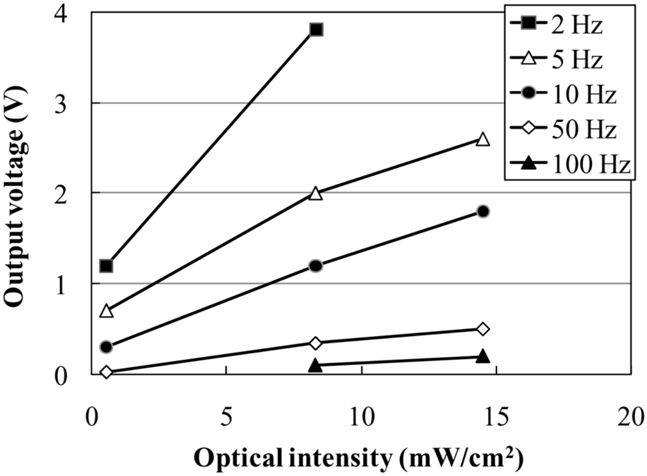

FIGURE 7 The relationship between the output voltage (V_o) and the optical intensity of irradiated blue-light. The frequency of read-out circuit was changed from 2 to 100 Hz.

of 25 mV for the difference between a steady state and a zero level. As a result, the resistivity of 250 Ωcm and the RC time constant of approximately 920 μs were obtained. Therefore, the RC time constant is not so large to affect the frequency response of the device [15].

We show in Figure 7, the relationship between the output voltage (V_o) and the intensity of irradiated light. The modulated read-out signal was ranged from 2 to 100 Hz, and the bias voltage (V_b) was applied to the device during the measurement. The output voltage increased with increasing the intensity of irradiated light. In such an organic photoconductive device, the photo-induced carriers are detected as the output voltage, and the photo-induced carriers increased with increasing the irradiated optical intensity. Therefore, the high intensity light causes more carriers in the organic photoconductive layer, resulting in the higher photocurrent [11,12].

The frequency dependence of the output voltage is shown in Figure 8. The intensity of irradiated blue-light was 0.6, 8.3, and 14.5 mW/cm^2, respectively. In all the cases, the output voltage decreased with increasing the frequency of read-out signal. This is because that the higher frequency read-out operation reduces photo-generated carriers in the organic photoconductive layer because of the low carrier mobility of F8BT compared to semiconductor materials [21,22] and the large gap between highest unoccupied molecular

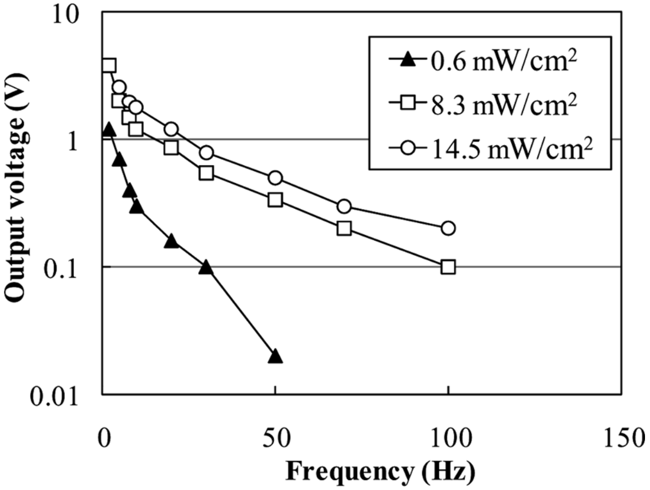

FIGURE 8 The frequency dependence of the output voltage (V_o). The optical intensities of irradiated blue-light were 0.6, 8.3, and 14.5 mW/cm^2, respectively.

orbital/lowest occupied molecular orbital levels of F8BT and work functions of electrodes [20,24,25]. However, the result indicates that the output voltage is still high enough up to 30 Hz for actual TV frame rates. In the frequency region of less than 30 Hz, more than 0.1 V could be detected as the photocurrent.

CONCLUSION

We investigated the read-out frequency response of a solution-processed organic photoconductive device in combination with the read-out circuit. The transient photocurrent showed enough frequency response for practical application of TV frame rates using organic photoconductive materials based on a wet process.

REFERENCES

[1] Nakano, S., Sekitani, T., Yokota, T., & Someya, T. (2008). *Appl. Phys. Lett.*, *92*, 053302.

[2] Hauch, J. A., Schilinsky, P., Choulis, S. A., Childers, R., Biele, M., & Brabec, C. J. (2008). *Sol. Energy Mater. Sol. Cells*, *92*, 727.

[3] Wang, D., Gong, X., Heeger, P. S., Rininsland, F., Bazan, G. C., & Heeger, A. J. (2002). *PNAS*, *99*, 49.

[4] Tatemichi, S., Ichikawa, M., Kato, S., Koyama, T., & Taniguchi, Y. (2008). *Phys. Sta. Sol. (RRL)*, *2*, 47.

[5] Shakutui, M., Fujita, K., & Tsutsui, T. (2006). *Jpn. J. Appl. Phys.*, *45*, L790.

[6] Kubota, H., Miyaguchi, S., Ishizuka, S., Wakimoto, T., Funaki, J., Fukuda, Y., Watanabe, T., Ochi, H., Sakamoto, T., Miyake, T., Tsuchida, M., Ohshita, I., & Tohma, T. (2000). *J. Lumi.*, 87–89, 56.

[7] Hagemann, O., Bjerring, M., Nielsen, N. C., & Krebs, F. C. (2008). *Sol. Energy Mater. Sol. Cells*, *92*, 1327.

[8] Brabec, C. J., Sariciffi, N. S., & Hummelen, J. C. (2001). *Adv. Funct. Mater.*, *11*, 15.

[9] Matsushita, Y., Shimada, H., Miyashita, T., Shibata, M., Naka, S., & Okada, H. (2005). *Jpn. J. Appl. Phys.*, *44*, 2826.

[10] Kawaguchi, H., Iba, S., Kato, Y., Sekitani, T., Someya, T., & Sakurai, T. (2005). *IEEE Sensors Journal*, *6*, 1209.

[11] Aihara, S., Hirano, Y., Tajima, T., Tanioka, K., Abe, M., Saito, N., Kamata, N., & Terunuma, D. (2003). *Appl. Phys, Lett.*, *82*, 511.

[12] Seo, H., Aihara, S., Watabe, T., Ohtake, H., Kubota, M., & Egami, N. (2007). *Jpn. J. Appl. Phys.*, *46*, L1240.

[13] Tang, C. W., VanSlyke, S. A., & Chen, C. H. (1989). *J. Appl. Phys.*, *65*, 3610.

[14] Vincentt, P. S., Barlow, W. A., Hann, R. A., & Roberts, G. G. (1982). *Thin Solid Films*, *98*, 171.

[15] Wei, B., Furukawa, K., Amagi, J., Ichikawa, M., Koyama, T., & Taniguchi, Y. (2004). *Semicond. Sci. Technol.*, *19*, L56.

[16] Kajii, H., Tsukagawa, T., Taneda, T., & Ohmori, Y. (2002). *IEICE Trans. Electron., E85-C*, 1245.

[17] Kim, J.-S., Kajii, H., & Ohmori, Y. (2006). *Thin Solid Films*, *499*, 343.

[18] Culligan, S. W., Chen, A. C.-A., Wallace, J. U., Klubek, K. P., Tang, C. W., & Chen, S. H. (2006). *Adv. Funct. Mater.*, *16*, 1481.

[19] Fukuda, T., Ohashi, M., Wei, B., Okada, T., Ichikawa, M., & Taniguchi, Y. (2007). *Opt. Lett.*, *32*, 1150.

[20] Fukuda, T., Wei, B., Ichikawa, M., & Taniguchi, Y. (2007). *Jpn. J. Appl. Phys.*, *46*, 7880.

[21] Chua, L.-L., Zaumeil, J., Chang, J.-F., Ou, E. C.-W., Ho, P. K.-H., Sirringhaus, H., & Friend, R. H. (2005). *Nature*, *434*, 194.

[22] Campbell, A. J., Bradley, D. D. C., & Antoniadis, H. (2001). *Appl. Phys. Lett.*, *79*, 2133.

[23] Barth, S., Müller, P., Riel, H., Seidler, P. F., & Rieß, W. J. (2001). *Appl. Phys.*, *89*, 3711.

[24] Niu, Q., Zhou, Y., Wang, L., Peng, J., Wang, J., Pei, J., & Cao, Y. (2008). *Adv. Mater.*, *20*, 964.

[25] Kim, Y., Cook, S., Choulis, S. A., Nelson, J., Durrant, J. R., & Bradley, D. C. C. (2004). *Chem. Mater.*, *16*, 4812.